Fractal Pattern Characterization of Acoustic Emissions For Continuous Damage Assessment of Reinforced Concrete Structures

Sui-Min (Simon) Hsiung[1]
Amitava Ghosh[1]
James Lankford, Jr[2]
Asadul H. Chowdhury[1], M. ASCE

Abstract

Many critical reinforced concrete structures and components undergo progressive damage because of the nature and magnitude of service loads, environmental effects, deterioration of material properties, and other factors. Depending on their locations, they may also experience major additional damage from natural disaster events such as earthquakes, hurricanes, high winds, and tornadoes. Continuous damage and structural assessment of these structures provides a mean for their possible timely repair and retrofitting for continuous use and operations. Research on brittle materials indicates that the microfracturing process (acoustic emission) is fractal in nature in both the temporal and spatial domains. The associated characteristics may serve as good indicators for continuous damage assessment and catastrophic failure prediction.

Introduction

When reinforced concrete structures are under stress from sustained as well as episodic loads, depending on the level of stress relative to their strength, microfractures form. Accumulation of microfractures may damage the structures and eventually lead to their failure. Often retrofitting and rehabilitation are required during the service life of a concrete structure so its reliability can be assured. However, the timing and extent of the required retrofitting and rehabilitation are difficult to determine. Ideally, the time and type of maintenance necessary should

---

[1] Center for Nuclear Waste Regulatory Analyses at Southwest Research Institute, 6220 Culebra Road, San Antonio, TX 78238-5166
[2] Southwest Research Institute, 6220 Culebra Road, San Antonio, TX 78238-5166

depend on the extent of damage. However, this information is typically unknown. Consequently, maintenance programs involving retrofitting and rehabilitation are often developed based on past experience on similar structures under similar conditions. This approach may lead to insufficient maintenance; and reduce the intended life or cause failure of structures.

Continuous monitoring of the damage pattern of critical concrete structures such as highway bridges, hydraulic dams, nuclear facilities, hospitals and other sensitive facilities would provide a deterioration history that could support rational decisions about timely retrofitting and rehabilitation of these structures. Currently, various approaches are in use (Smith, 1987; Crist and Kechter, 1987; Overman et al., 1987) for monitoring structural performance, each with its own advantages and disadvantages.

Among these techniques, acoustic emission (AE) techniques have been used widely in evaluating integrity of repaired reinforced concrete and assessing cracks forming in reinforced concrete under various loading conditions (Nippon Physical Acoustics, Ltd., 1999). Although field applications of AE techniques to concrete structures have been hampered because of the high attenuation of concrete (Landis et al., 1994), this difficulty may be overcome by strategically installing sensor networks in a relatively smaller region of interest. Under this premise, this paper explores the possibility of qualitatively assessing structural damage and providing early warning of catastrophic failure through fractal characterization of AE. Additional work will be needed to quantitatively assess structural damage using this technique.

Technique for Estimation of Structure Damage

Progressive fracturing processes of brittle materials under stress are known to be fractal and thus possess fractal characteristics at laboratory and field scales [e.g., in rock pillars or wall rocks near mine openings (Scholz, 1968a,b,c; Hirata, 1987, 1989; Hirata et al., 1987; Ghosh, 1990; Xie and Pariseau, 1993)]. An object or a process is said to be fractal when any part is similar to the whole when enlarged suitably to the same scale. This phenomenon suggests that fracturing processes of brittle materials are scale independent. Because of the unique scale-invariant feature of the fracturing process, the observations made from the laboratory experiments on small samples may be extended to a much larger structure in the field. Although the literature noted above is mostly related to rocks, the same phenomenon is expected in reinforced concrete structures, since the microfracturing processes for rock and concrete material are similar (Landis et al., 1994).

Studies have shown that individual microfracturing clusters in time. The scale-invariant Omori's law developed for aftershock sequences of earthquakes was found to be valid as well for laboratory measured acoustic emissions (Hirata, 1987; Scholz, 1968c; Xie and Pariseau, 1993). Similarly, the spatial distribution of microfractures in laboratory experiments (Hirata et al., 1987; Ghosh, 1990; Cox and Meredith, 1993), microfractures and rock bursts in mines (Xie and Pariseau, 1993), and fractures in rock masses (Ghosh and Daemen, 1993) have also been determined to have fractal structures. Tchalenko (1970) studied the fracture pattern produced under shear load at widely varying scales from laboratory specimens to earthquakes. He observed that the fracture pattern looked similar in both cases. He also observed that some of the individual fracture structures were similar to the main fracture pattern at a smaller scale (i.e., they had a self-similar fracture structure). Studies (Scholz, 1968c; Cox and Meredith, 1993) have also shown that the cumulative frequency of acoustic emissions in laboratory experiments that occur at a given magnitude follows the fractal distribution. These observations regarding time, location, and magnitude of microfracturing suggest that there is no characteristic size of the fractures formed. The fracturing process is fractal or scale-invariant and, consequently, possesses self-similar characteristics.

Because the fracturing process is dependent on stress field, material characteristics and related factors, the fractal dimensions and the fractal intercepts (prefactors) for different materials are expected to be different, although the process of microfracturing will remain the same with a self-similar fracture pattern. Furthermore, the fractal dimension of a fracture distribution does not remain constant as a structure is progressively damaged. Initially the fractal dimension increases with loading, indicating almost random formation of microcracks in the three-dimensional space. This phenomenon continues until the structure is close to failure; at which time an ultimate fracture plane begins to form through interaction and coalescence of microfractures, producing clusters both in space and time. Formation of the fracture plane leads to a decrease in fractal dimension. This indicates that the microcracks are no longer uncorrelated, but form a two-dimensional plane (macrofracture). Fractal dimension may increase if the loading continues beyond the preliminary fracture formation as microfracturing events associated with the formation of the secondary fractures are recorded.

In the study presented in this paper, the fractal characteristics of microfracturing in rock were analyzed to identify potential parameters that can be related to the extent of material damage and possibly timing and location of failure. Fifteen cylindrical Apache Leap tuff rock samples were used for uniaxial compression tests to monitor the microfracturing process during loading. The samples were relatively free of major visible flaws. The data collected from the AE acquisition system include counts (number and rate) of microfracturing events, and arrival time to the sensors generated by the formation of microfractures (Hsiung et al., 1999). The sampling was performed at a rate of 2 MHz for all tests. The level for the pre-amplifiers was set at 60 dB to amplify the signal, and trigger thresholds were varied from as low as 40 dB to as high as 80 dB in these tests to avoid interference from noises. Other data collected included uniaxial compressive stress, axial strain, and failure mode. The compressive tests were performed at a constant loading rate of 0.15 MPa/sec. Figure 1 shows a typical stress and accumulation of microfracturing events as a function of time. It can be observed that the applied stress is approximately linear and that microfracturing activity is small until more than half way through the test.

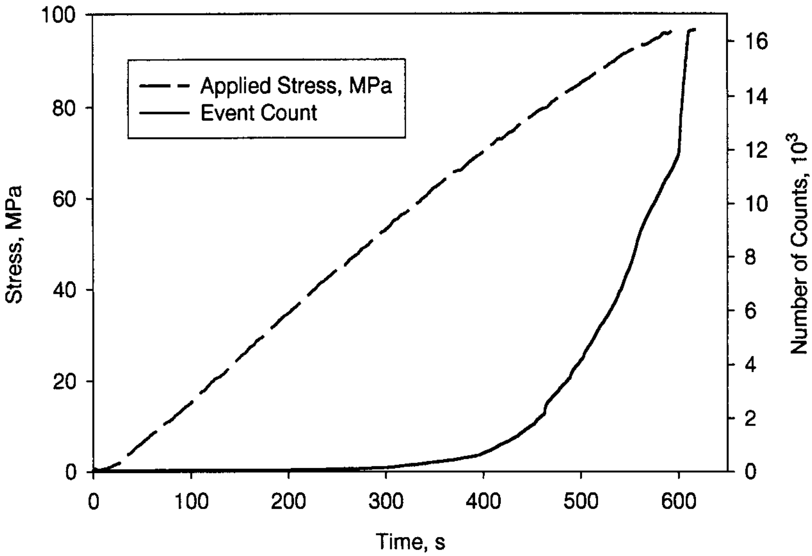

Figure 1 Applied stress and accumulation of microfracturing events with time for sample 18

Formation of microfractures is characterized in five-dimensions: time, three spatial dimensions, and magnitude. These characteristics are related to the stress field, rate of loading, and magnitude of stresses compared to the macrofailure strength of a material. If formation of individual microfracture is taken as a point process, this microfracturing phenomenon shows scale-invariant or fractal structure both in space and time. A similar scale-invariant phenomenon has also been observed with the energy release associated with microfracture formation. In this section, discussion will focus on analyzing microfracturing process in the temporal domain.

Fractal Clustering

In conducting the analysis, the fractal distributions are related to probability. The objective is to determine the probability that a predetermined time interval contains at least one microfracturing event for the duration of interest. The probability that a time interval t_n will include at least one event can be given by

$$p_n(t_n) = N_n(t_n)\frac{t_n}{t_D}, \quad \text{where } n = 1, 2, \ldots \tag{1}$$

where $N_n(t_n)$ is the number of time intervals that contain at least one event for the duration t_D. The time interval t_n can be arbitrarily chosen. The total number N_T of time intervals for t_D is t_D/t_n. When N_n is greater than or equal to N_T, p_n is equal to 1, which means that every time interval with a length of t_n includes at least one event. In conducting fractal analysis, t_n should be chosen such that $N_n < N_T$ so that variation of p_n can be analyzed to identify fractal pattern.

An object or a process is said to be fractal when any part is similar to the whole when enlarged suitably to the same scale; a fractal set can be defined as

$$N_n(t_n) = \frac{C}{t_n^D} \tag{2}$$

where C is a constant of proportionality or prefactor and D is the fractal dimension. Replacing $N_n(t_n)$ in equation (1) with that in equation (2), one can obtain

$$p_n(t_n) = C\frac{t_n^{1-D}}{t_D} \tag{3}$$

Both the fractal dimension and prefactor can be determined by curve fit equation (3). Equation (3) is used in our study of microfracturing process in a rock sample under compression.

Characteristics of Temporal Distribution of Acoustic Emission

Fourteen AE data sets from fourteen samples were analyzed to study fractal clustering in the temporal domain throughout the test duration. Note that the terms AE and microfracturing events are used interchangeably in this paper. The fractal analyses were performed in a discrete manner, that is, at a predetermined time/load increment (e.g., every 0.1% to 1% time/load increment). The data set used for each fractal analysis contains the microfracturing events from the beginning of the test to each specified time. For example, at time t_1, the microfracturing events occurred between the beginning of the test (time t_0) to t_1 were analyzed to determine the fractal characteristics and at time t_2 for $t_2 > t_1$, the data set from time t_0 to t_2 is used. This approach is referred to as time progression in this study. A progression time step is defined as the time difference between two consecutive specified times (e.g., $t_2 - t_1$). The fractal characteristics were plotted against time to examine their temporal variations. The time interval set selected for analyzing fractal clustering of each data segment of the microfracturing process for each experiment in this study is 1.5^n where n = -20, -19, ..., -4. The choice of the time interval is somewhat arbitrary. However, the time interval selected here gives an equal time spacing in the logarithm space that will ensure better regression results.

Figure 2 compares the effect of number of steps of time progressions on fractal dimension and prefactor calculated for sample 19. In this figure, the fractal dimension and prefactor are displayed as functions of time. The solid lines with symbols indicate the fractal characteristics calculated based on 40 time progression

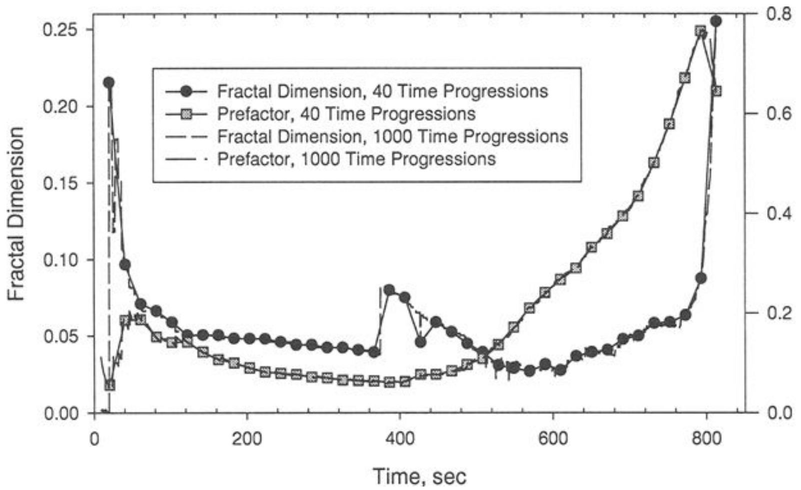

Figure 2 Effect of number of time progressions on variation of fractal characteristics of a microfracturing process for sample 19

steps, while the dash lines without symbols are for 1,000 time progressions. Other than some differences at the beginning of the test, the general trend for the variations of the fractal characteristics with time for sample 19 is essentially the same regardless of the number of time progressions used for the analysis. This observation suggests that the fractal characteristics for the temporal distribution of the microfracturing events are relatively insensitive to the number of time progressions used; they are not affected by the size of the progression time step. Similar behavior is also observed for other test results analyzed. The insensitivity of the fractal characteristics to a wide range of progression time steps gives reasonable assurance that the analysis technique will work. However, the progression time step cannot be too large or the number of time progressions too small such that major "localized" clustering will be included in just one time progression. In such cases, capturing the variation of fractal characteristics for the microfracturing process in the temporal domain may not be possible. Although preliminary analysis of the available data should provide a good indication of the possible range of progression time steps that can be used, the progression time step should be as small as possible so that changes in fractal features can be identified in a timely manner as fracturing develops.

In this study, microfracturing events are detected in some of the samples at the early stage of the test (Hsiung et al., 1999). Formation of microfractures at an early stage of loading (low stress) is likely related to the inherent weakness of the material. Once this weakness-related microfracturing is completed, microfracturing activity diminishes substantially. However, in the remaining samples, microfracturing at the early stage of testing is almost absent, indicating that the material could be relatively free of inherent weakness. In our study, clustering of microfractures at the later stage of testing is of greatest interest. For all the test results analyzed, it is observed that fractal dimension and prefactor do not significantly increase until the applied stress is at least about 40% to 50% of the material strength. In some cases, no significant increases are observed until the applied stress reaches 60% to 70% of the material strength. As discussed earlier, the increase in fractal dimension and prefactor are closely related to the intensity of the microfracturing activities; thus such an increase may be used to indicate damage level.

As the test progressed toward failure of the sample, fracture planes began to form. Either the fractal dimension or prefactor started and continued to decrease until the sample failed for all but one sample. However, it appears that no single dominant parameter can be consistently used to describe the microfracturing processes for all the samples tested, even though these samples are of the same rock type. For example, the fractal characteristics seem to be quite different for samples 8 (Figure 3) and 18 (Figure 4). In both cases, the fractal dimension and the prefactor begin to decrease at the later part of the test. For sample 8, the fractal dimension started to decrease relatively early, at about 73% of the test duration, as compared to the time of sample failure and the prefactor started to decrease right before the failure of the sample. However, the trend is reversed for sample 18; the prefactor started to decrease at about 75% of the test duration and the fractal dimension started to decrease right before the failure of the sample. For some test cases, only one of the fractal characteristics shows sign of decreasing. It is also worth noting that the lead-times for the fractal characteristics vary substantially. The lead-time is defined here as the time difference between the time that a fractal characteristic reaches a peak

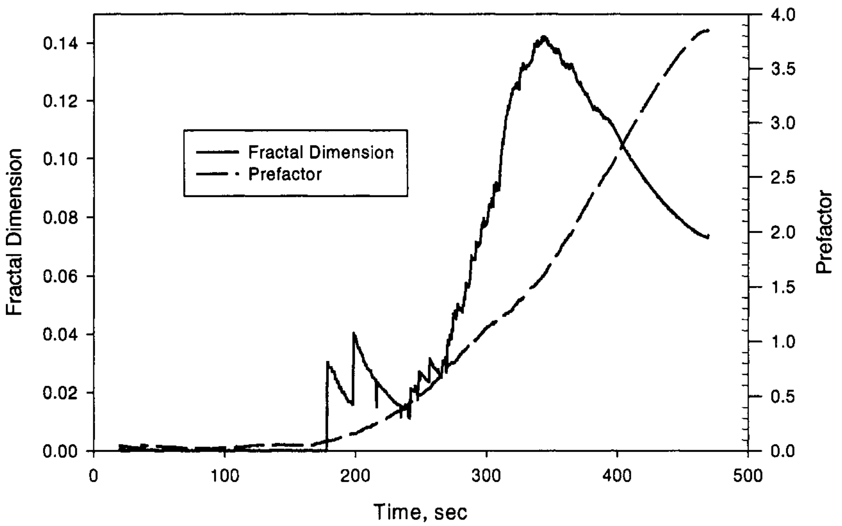

Figure 3 Variation of fractal characteristics of the microfracturing process for sample 8

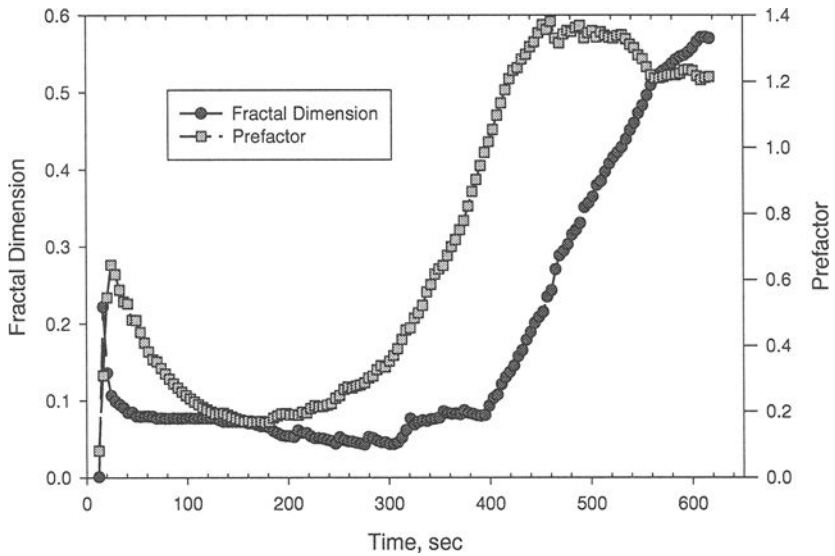

Figure 4 Variation of fractal characteristics of the microfracturing process for sample 18

value and the time that the sample fails. These observations reinforce the notion that the microfracturing process is unique for each sample, even if the samples are of the same material.

Table 1 lists the lead-time for the fractal characteristics of each sample. The lead-time listed in the table is normalized using the total test time required to fail the sample and presented in percentage. The existence of a lead-time between the time of a peak fractal dimension or prefactor and the time of material failure makes it possible to use this fractal characteristic as a precursor for failure prediction. As can be seen from Table 1, for more than half of the test results, only one fractal characteristic possesses a lead-time. Also, the lead-times for fractal dimensions identified for samples 10, 11, and 14 are too long, meaning that the fractal dimension begins to decrease too early relative to the actual time of failure. This behavior may be related to the early formation of fracture planes that were not sufficient to coalesce into major fracture planes that fail the samples; consequently, the microfracturing process continued. This behavior, on the other hand, may serve as a good indicator for assessing structural damage. This information in conjunction with the information on locations of microfracture clustering should provide valuable insight regarding the need for maintenance of concrete structures. However, with these long lead-times, the associated fractal dimensions would not be appropriate for forecasting material failure. If this is the case, the corresponding lead-times for prefactors may be used as a precursory parameter. For samples 10, 11, and 14, the lead-time for prefactor is relatively short. These short lead-times may be problematic in the sense of providing early warning for structure failure if they do not allow sufficient time for identifying the peak value before failure. Although a short warning time for structure failure may not be ideal, it is better than no warning at all.

Characteristics of Spatial Distribution of Acoustic Emission

It has been observed that the spatial distribution of event source locations estimated within the rock samples possesses a multifractal distribution. For homogeneous fractals, a unique fractal dimension is sufficient to describe the self-similar characters. However, most fractal objects in nature and dynamical systems are not homogeneous, rather heterogeneous (Mandelbrot, 1989).

Table 1 Normalized lead-time when the fractal characteristics show sign of decreasing before sample failure

Sample No.	Prefactor	Fractal Dimension	Sample No.	Prefactor	Fractal Dimension
7	0.3%	17.7%	16	0.24%	No**
8	0.1%	26.8%	17	0.23%	No*
9	No*	16.4%	18	25.1%	1.0%
10	0.1%	40.3%	19	2.2%	No*
11	0.3%	52.5%	20	1.8%	No*
14	0.1%	40.1%	21	5.9%	No*
			22	No*	11.1%

Note:
* No sign of decreasing (no lead time)
** A local peak is observed. The associated lead-time is about 12.3%

A single dimension is not sufficient to characterize the fractal properties of such objects or phenomena. The idea of fractal dimension (monofractal analysis) has been extended for such characterization (multifractal analysis). A monofractal analysis only provides information on the support of a set for a given measure. However, it does not provide any insight into the distribution of the measure on its support (Ouillon and Sornette, 1996). Multifractal analysis describes the scale-invariant characteristics of the measure itself and was used for analyzing the spatial distribution of microfractures.

Source Location Determination

Before the spatial distribution of the microfractures can be analyzed using the multifractal approach, source locations of the events need to be determined. In this study, two algorithms were examined for determining the source locations of microfracturing events.

The first algorithm involves adopting a least-squares scheme to minimizing the errors associated with the predicted source location of an event as suggested by Blake et al. (1974). This algorithm recognizes the uncertainties associated with the measurement of arrival times and heterogeneity of the rock medium. The least-squares technique attempts to minimize the influence of random errors associated with these uncertainties. The random errors are represented as the perpendicular distances from some point $P_1(x_c, y_c, z_c)$ in space to each plane described by the linear equations (more discussion regarding the linear equations is provided in the following paragraphs). Minimization is performed on the sum of the squares of these distances with respect to point P_1, which produces a best-fit source location. This technique requires at least five sensors/transducers and, in general, the more sensors used the better the solution.

The second algorithm to determine source location involves minimizing errors associated with the predicted travel times from event location to sensors. The approach suggested by Lockner and Byerlee (1980) and Lockner et al. (1992) was adopted. This algorithm calls for inversion of the relative arrival time for determining source location and event initiation time. A least-squares technique is employed to estimate source locations by minimizing errors associated with the travel times through an iterative procedure.

Lockner and Byerlee (1980) showed that progressive deformation and fracturing of the sample under compression could lead to velocity field heterogeneity. They suggest that the velocity anisotropy may be approximated by $\xi = V^{transverse} / V^{axial}$, and generally decreases from 1 to less than 0.6 as the sample is loaded (Lockner and Byerlee, 1980; Lockner et al., 1992). This effect was accounted for in both algorithms for source location determination (Hsiung et al., 1999).

Velocity of propagation of a p-wave from an acoustic event through a medium is an important parameter in determining source locations for acoustic events. The p-wave velocity is, in turn, closely tied to the Young's modulus of the medium in which the wave is propagating. The relationship between the p-wave velocity, V_p, and medium Young's modulus, E, can be expressed as

$$V_p = \sqrt{\frac{E(1-\nu)}{(1+\nu)(1-2\nu)\rho}} \tag{4}$$

where ν is the Poisson's ratio and ρ is the density of the medium. Figures 5 show plots of V_p and E versus time. Since the variation in V_p could be as large as 40%, it is important to include this effect in the determination of event source location.

Assuming that the arrival times are accurately recorded and the p-wave velocity in the sample is known, prediction of source locations using Algorithm 2 (minimizing errors with travel time estimation) is, in general, slightly better than Algorithm 1 (minimizing errors with source location estimation).